frontiers | Frontiers in Earth Science

TYPE Original Research
PUBLISHED 20 August 2025
DOI 10.3389/feart.2025.1607126

OPEN ACCESS

EDITED BY
Abani Kumar Patra,
Tufts University, United States

REVIEWED BY
Hongchao Dun,
Lanzhou University, China
Morgane Jolivet,
Tour du Valat, France

*CORRESPONDENCE
David M. Kennedy,
davidmk@unimelb.edu.au

RECEIVED 07 April 2025
ACCEPTED 29 July 2025
PUBLISHED 20 August 2025

CITATION
Kennedy DM, Yuan R, McCarroll RJ, Liu J, Beetham E and Ierodiaconou D (2025) Shoreline dynamics of an urbanised estuarine beach under the influence of changing sediment budgets.
Front. Earth Sci. 13:1607126.
doi: 10.3389/feart.2025.1607126

Shoreline dynamics of an urbanised estuarine beach under the influence of changing sediment budgets

David M. Kennedy[1]*, Runjie Yuan[1], R. Jak McCarroll[2], Jin Liu[2], Eddie Beetham[3] and Daniel Ierodiaconou[4]

[1]School of Geography, Earth and Atmospheric Sciences, The University of Melbourne, Parkville, VIC, Australia, [2]Regional Coastal Adaptation and Planning, Department of Energy, Environment, and Climate Action, East Melbourne, VIC, Australia, [3]Tonkin and Taylor Ltd., Auckland, New Zealand, [4]School of Life and Environmental Sciences, Deakin University, Warrnambool, VIC, Australia

Sandy beaches within estuaries and bays are dynamic landforms. As many large urban centres are located on the margins of these enclosed marine systems the beaches that form their shoreline are often subject to significant management intervention. Understanding the geomorphological evolution of these beaches and their future evolutionary pathways is therefore difficult as it requires detangling human modification of sediment budgets from natural variability. In this study, a multiproxy shoreline analysis is undertaken of a 3 km long fetch-limited beach in Port Phillip Bay, Australia. The beach is divided into several sediment compartments delineated by groynes and natural rocky outcrops, each exhibiting shoreline rotation on the seasonal scale leading to lateral profile movement of up to 40 m. The medium-term (last 30 years) sediment budget is approximately +3,000 m^3/year due to longshore drift and nourishment. Beach nourishment over the last 40 years accounts for 25% of the total sediment budget. This has balanced the loss of natural sediment supply from cliff erosion caused by erosion protection works such as seawalls. It is concluded that groyne construction has enhanced shoreline rotation patterns on a seasonal scale. Overall, this study shows how human modifications to the sediment budget were initially negative but now maintain a functioning geomorphic environment. Full consideration of the seasonal-scale shoreline dynamics is required to understand longer (decadal-scale) beach evolution.

KEYWORDS

estuarine beach, Port Phillip Bay, longshore transport, nourishment, compartments, drones, shoreline proxy

1 Introduction

Beaches within estuaries and bays (BEBs) are dynamic systems that are often neglected in research due to a perception that they are simply scaled down versions of open-ocean systems (Jackson et al., 2017; Nordstrom and Jackson, 2012; Vila-Concejo et al., 2020; Vila-Concejo et al., 2024). While their energy environment is often lower than on coasts directly exposed to deep-water ocean waves, modelling their response to sea-level rise is difficult as their morphology and dynamics are strongly related to local-scale boundary conditions. For example, many may only be active during high-energy events rather than

modal conditions, especially deep inside the estuarine basin away from the open-ocean entrance (Goodfellow and Stephenson, 2005; Kennedy, 2002; Gallop et al., 2020; Costas et al., 2005). Those connected to major sediment sources such as flood-tide deltas (Fellowes et al., 2021; Gallop et al., 2020; Bittencourt et al., 2001) are more able to adjust their profile to changing energy conditions compared with those dependant on highly localised sediment sources such as cliff erosion (Jackson et al., 2002; Vila-Concejo et al., 2020).

Human development on the margins of estuaries and bays also adds additional complexity to understanding future behaviour (Nordstrom, 1992). The shorelines of urbanised beaches are often highly developed with sea walls, groynes, pipes and other hard structures dominating the intertidal zone (Nordstrom, 1989; Bird and Lewis, 2014; Kennedy et al., 2025). In many cases, beaches are constructed, or nourished, as 'nature-based' coastal defence (Morris et al., 2019; IUCN, 2020; Chen et al., 2022) as well as to create new recreational resources (Hanson et al., 2002). The result is many BEB's can be considered to be artificial, with their morphology a product of deliberate or unintended management actions.

As urban areas grow, the degree of management intervention into the littoral zone scales through time with development. For understanding contemporary beach dynamics, it therefore becomes necessary to view morphologic behaviour in the context of a history of human modification, both deliberate and unintentional. In this study, we explore the morphodynamics of a highly managed temperate sandy beach in order to understand the tipping points of these vulnerable geomorphic systems through time. Using a fetch-limited system in Port Phillip Bay, southeastern Australia, we aim to understand how the contemporary beach movement is determined by present and past management activity. The aim is to assess the impact of increased human intervention on shoreline behaviour in order to determine how changing management priorities have affected shoreline movement. We use a case-study approach as an example of one pathway of beach behaviour. Such information is critical in the context of greater uncertainty with climate change and population growth which is expected to impact estuarine environments to a greater degree than open-ocean coasts in the future (Vila-Concejo et al., 2024).

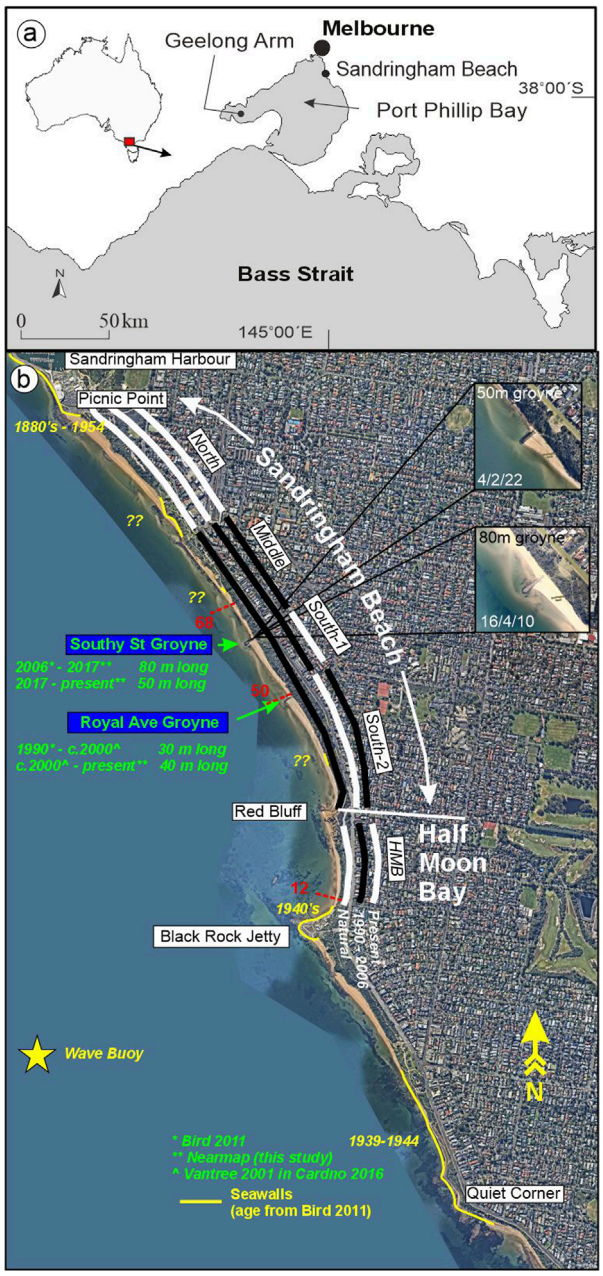

FIGURE 1
(a) Location of Sandringham Beach within Port Phillip Bay on the southern, temperate margins of the Australian continent. **(b)** Aerial images of the Sandringham embayment showing the major phases of hard coastal management in the past 150 years and their timing (green and yellow text). The black-white rectangles provide a visual delineation of the sub-compartments through time. The construction of groynes has led to progressive subdivision of the embayment into many sub-compartments, especially since 1990. The position of the wave buoy (data in Figure 3) and examples of transects (red text) (data in Figure 7) are also mapped.

2 Regional setting

Sandringham Beach is a 3 km long sandy system (centred at 37°57′25.47″S, 145° 0′23.61″E) located on the northeastern edge of Port Phillip Bay, Victoria, Australia (Figure 1a). The Sandringham embayment is composed of two tertiary-scale sediment compartments, Sandringham Beach and Half Moon Bay, separated by a rocky promontory (Red Bluff, see Figure 1b) (Kennedy et al., 2025). The beach is found at the base of cliffs (up to 30 m high) formed in sandstones and conglomerates of late Miocene to early Pliocene age (VandenBerg, 2016).

Port Phillip Bay is an enclosed estuary 54 km long (north-south) and 32 km wide, extending to 56 km width through the Geelong Arm (Figure 1a). The bay floor is on average 9–24 m deep and shallows to <5 m depth within 12 km of its bedrock-defined entrance at its southern edge (Dalby et al., 2024). Tides are microtidal, with a mean spring tide range of 1.4 m at the bedrock-defined entrance, decreasing to 0.9 m further inside the bay (PoM, 2013). Waves near the entrance have a mean significant height (H_s) of 1.0–1.5 m, but they do not propagate far inside the estuary past the limit of the floodtide delta. The majority of the bay is fetch-limited dominated by seasonal wind patterns (Goodfellow

and Stephenson, 2005; Bird, 2011; Kennedy et al., 2023; Lowe and Kennedy, 2016) with mean annual H_s of <0.5 m in the Sandringham region (Tran et al., 2021). Winds are predominantly southerly in the austral summer and northerly in winter. The 100-year return period storm tidal elevation at Sandringham is 1.07 m (Tran et al., 2021).

Sandringham Beach has been subjected to major management interventions for over a century (Figure 1b). At the northern and southern ends of the compartment, harbours, seawalls and breakwaters were constructed from the 1880's with a major phase of seawall construction occurring in the 1930's and 1940's (Figures 1b, 2a). Further to this, the bluffs behind the beach have been buried in building waste presumably to infill old gullies likely similar in form to the current face of Red Bluff or the rear of the Middle sub-compartment (Figures 2b,c). The result of these actions is the eroding cliffs can no longer be considered a significant source of beach sediment.

Intentional interference with longshore sediment transport occurred in 1990 (opposite Royal Ave) in the form of a 30 m long rock groyne which was extended to 40 m between 1990 and 2010 (Figure 1b). A second rock groyne 80 m long was constructed in 2006 at Southy St, later shortened to 50 m in 2017 (Figure 2c). The hard structures of groynes and rocky outcrops define five sub-compartments within the embayment (North, Middle, South-1, South-2 and Half Moon Bay (HMB)) (Figure 1b). Nourishment projects have occurred concurrently with groyne construction, focussed on specific sub-compartments, rather than the entire beach at one time (Table 1). The first recorded was in 1986, with further projects in 1993, 2009, 2018 and 2021.

3 Methodology

Shoreline change was analysed from aerial imagery using a vegetated and wetted lines proxy. The vegetation line, defined as the seaward limit of plant growth, was considered to represent the longer-term position of the shoreline and exclude short-term tidal and storm surge dynamics (Burningham and Fernandez-Nunez, 2020), however it is acknowledged that the active management at the site means a natural equilibrium between plant growth and sedimentation is unlikely to occur. This means the vegetation lines can often correspond to the position of artificial structures such as seawalls. The wetted line, defined by the change in colour of sand resulting from wave and tidal inundation, represents an instantaneous shoreline at the time of image acquisition (see Boak and Turner (2005); Pajak and Leatherman (2002) for a review of these proxy methods). A vertical elevation of 0.5 m AHD which is approximately the location of mean high water spring (MHWS) tide elevation has previously been used to delineate the shoreline by the Victorian Government Department of Energy, Environment and Climate Action, to streamline shoreline analyses. This study also tested the reliability of this delineation using Digital Surface Models (DSM's) produced through Unoccupied Aerial Vehicle (UAV) surveys.

Historical aerial images were obtained from the Victorian Government, spanning 93 years from 1930 to 2023. Vegetation and instantaneous waterlines were manually extracted from the georectified imagery. No tidal correction was applied. The minimum horizontal resolution of older images (pre-2000) is 0.5 m, with a maximum of 0.1 m for newer images (2010 onward). An independent georectification (Carvalho et al., 2020) of images from the same dataset determined a root mean square error (RMSE) of ≤1 m for images from 1960 onwards and due to the same workflows being conducted in this study we assume that older images have a similar RMSE. Based on a comparison with that dataset, we conservatively estimate an uncertainty of ±3 m for the extracted vegetation lines based on vectorisation and image errors. All shorelines measured are referenced to the 2019 a tidally-adjusted annual mean wet-dry line extracted from Digital Earth Australia (DEA) (DEA, 2022; Bishop-Taylor et al., 2021). The 2019 shoreline was selected as shadows from the cliffs behind the beach, meant many of the shorelines in the DEA database were incorrect. The DEA shorelines have a Mean Absolute Error (MAE) of 7.3 m and RMSE of 10.3 m (DEA, 2025).

UAV surveys, using a DJI Phantom 4 Pro and RTK models, with RTK-GPS ground control points, were undertaken every 6–8 weeks from April 2020 until May 2023 with a vertical and horizontal accuracy (RMS error) of 0.11 and 0.02 m respectively (see Pucino et al. (2021); Ierodiaconou et al. (2022) for methodological and quality assurance details). All imagery was processed into digital surface models using Structure-from-Motion techniques (Westoby et al., 2012). For all aerial datasets, transects at 30 m spacing were cast across all time steps to analyse shoreline change. Rates of change in shoreline position were calculated based on linear regression of the entire dataset. Further details on the method of integration of UAV and satellite datasets for coastal management can be found in McCarroll et al. (2024).

Concurrent with the UAV surveys, a SOFAR Spotter wave buoy was deployed in approximately 10 m water depth, 1.6 km offshore southwest of Black Rock Jetty (Figure 1b). The buoys use high-resolution GPS to measure its vertical and horizontal motion. This 3D motion time series was processed using the Fast Fourier Transform (FFT) to generate the wave energy spectrum, from which significant wave height, wave period, and wave direction are derived. These wave parameters are transmitted to remote servers and visualized via a user dashboard. In this study, the bulk wave parameters were directly obtained from AUSWAVES (https://auswaves.org/), a national platform for wave observation and data sharing.

To calculate sediment budgets, shoreline position (wetted-line) was used to determine active profile volume. This was completed using the assumptions of equilibrium profile shape, depth of closure and active profile height (for full details see (McCarroll et al., 2021; Harley et al., 2022; Dean and Houston, 2016) (See Supplementary Table S1). As a general rule shoreline change (δX) is a function of the volumetric change (δV) and height of the active profile (h_a). The depth of closure was estimated from Hallermeier (1980)) combined with examination of single beam echosounding profiles perpendicular to the field site. Volume may be expressed as per unit alongshore (m^3/m) or as a total volume (m^3) by integrating alongshore.

$$\delta X = \delta V / h_a \quad (1)$$

10.3389/feart.2025.1607126

FIGURE 2
(a) Terrestrial grasses and shrubs on an engineered slope behind a seawall at Melrose St (North). **(b)** Shrubs, small trees and grass on the engineered slope at the southern end of the beach viewed from Red Bluff Lookout (South-2). **(c)** Active gullies in the old sea cliff behind Sandringham Beach. Only a few examples of this original geomorphology remain, preserved to show the natural condition of the area. **(d)** The Southy Street Groyne shows beach accumulation on its southern side.

TABLE 1 Historical details of renourishment activities undertaken in the Sandringham embayment. Updated from Cardno (2016).

Completion Date (sub-compartments)	Beach Length (km)	Volume (m^3)	Sediment Source	Nourishment Sand Size
August 1986[a]	0.4	No data	No data	No data
1993 (South-2)	0.6	16,000	No data	>1.0 mm
2009 (South-1)	0.5	12,500	No data	No data
2018[b]	0.2	2,830	Birdons near Sandringham Harbour	Fine/Medium
May - July 2021 (South-2)	0.3	11,909	>10 m depth, 800 m WNW of Black Rock Jetty	Fine/Medium
May - July 2021 (HMB)	0.1	1,078	>10 m depth, 800 m WNW of Black Rock Jetty	Fine/Medium

[a]The precise location of this renourishment is unknown and may be Quiet Corner and Watkins Bay, adjacent to Black Rock rather than in the Sandringham Embayment (Bird, 1990; Bird, 2011).
[b]The precise location of this renourishment may be to Hampton Beach.

4 Results

4.1 Shoreline proxies from UAV-imagery

To test the use of time series combining UAV and aerial imagery shoreline proxies, a statistical test was applied to determine the total uncertainty bounds for shorelines derived from these two methodologies. The average time offset between the two datasets is 11.6 days during a period of negligible wave activity and therefore little to no reworking of the profile was assumed. Horizontal uncertainty for the UAV shoreline proxy is +/- 1 m (based on 0.1 m vertical uncertainty and assuming a 1-in-10 beach slope). The UAV shoreline proxy was assumed to be more precise than the aerial shoreline proxy. This is because the aerial imagery was not tidally corrected due to the hourly-scale timing of acquisition being unknown and therefore it has unconstrained uncertainty prior to this test. A vertical elevation of 0.5 m above mean sea level (MSL) has previously been used to delineate the shoreline in the region as it is equivalent to MHWS elevation and is also the lowest vertical elevation common to all surveys (CoastKit, 2023). There is an overlapped surveying period (from December 2020 to September 2021) covered by these two datasets within which the UAV surveys were undertaken at five different dates. Shoreline positions in the aerial imagery obtained close to the UAV survey dates were then interpolated to estimate the instantaneous wet/dry shorelines in the same dates. By comparing the 0.5 m datum against the interpolated digitised shorelines of the aerial imagery, there is a good relationship between the two methods of shoreline delineation ($r^2 = 0.9$) based on the data used in this exercise.

4.2 Seasonal wave dynamics

The mean significant wave height recorded offshore of the Sandringham Embayment from April 2021 to March 2023 was 0.40 m, with a mean wave period of 2.71 s and a mean SW direction of 234.1° (Figure 3). Notably, the significant wave height exhibits apparent seasonality. The significant wave height reaches its maximum (~0.45 m) in February, November, and December and its minimum (~0.35 m) in May, July, and August (Figure 3). This pattern suggests that wave conditions are primarily influenced by the local weather systems. From May to August, wave directions are bimodal, with waves originating from the NNW and WSW. In December, waves predominantly come from the SWS, indicating a relatively narrow directional spread. During other seasons, waves exhibit a broader range of directions.

In summer (October–March), the mean significant wave height was slightly higher at 0.43 m, with a mean SSW–SW direction of 219.1°. In winter (April–September), a lower mean significant wave height of 0.37 m was recorded, with an average WSW direction of 252.5°. However, it is important to note that the wind direction remains bimodal throughout winter. No clear seasonal trends were observed in wave period.

4.3 Historical shoreline change (1930–2023)

To understand the trends in shoreline position, an average of all transects taken within sub-compartment was undertaken and analysed with respect to the position of the wetted line in the oldest imagery (Figure 4). Through taking a mean value of all transects, the impact of seasonal variation is reduced thereby allowing better identification of decadal trends, as the seasonal pattern roughly balances itself within each sub-compartment. Overall, the beach at Sandringham was dynamic, but generally stable to accreting over the past 93 years, within the bounds of image uncertainty. HMB and North are 2 and 7 m wider today, while South-1 is 3 m narrower. The Middle sub-compartment is clearly erosional.

High magnitude variations in the wetted line position were common before 1980. This was particularly noticeable in the 1960's with major retreat (>20 m in places) in 1960, followed by rapid accretion in 1963, except at HMB (Figure 4). The shoreline fluctuations were subsequently at magnitudes of ±5 m until the

10.3389/feart.2025.1607126

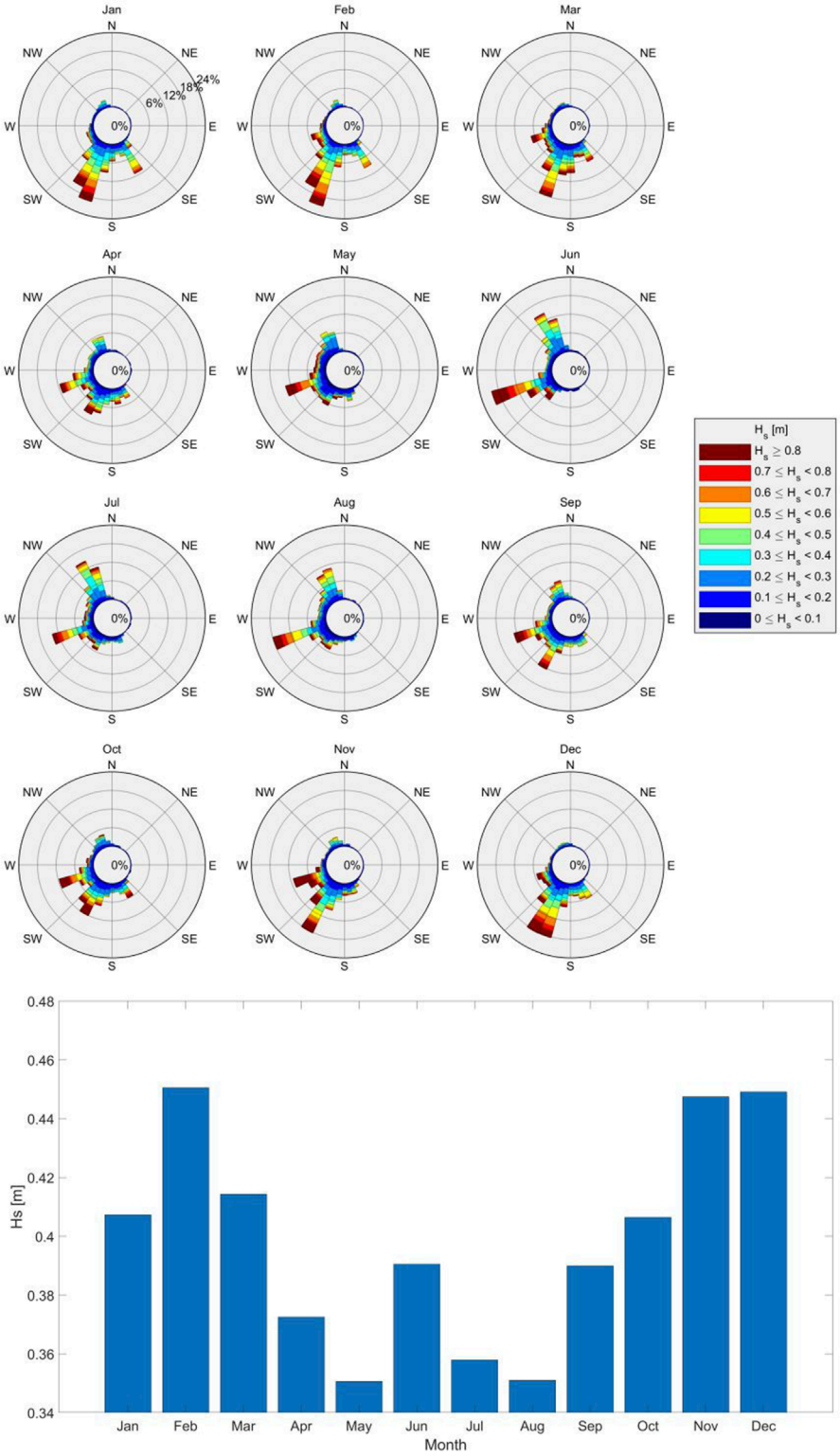

FIGURE 3
Wave roses for measured offshore of Sandringham Beach at 10 m water depth from 2020 to 2023 recorded by a Soffar Spotter™ buoy and mean significant wave height for each month during the data collection period. Data available through https://auswaves.org/.

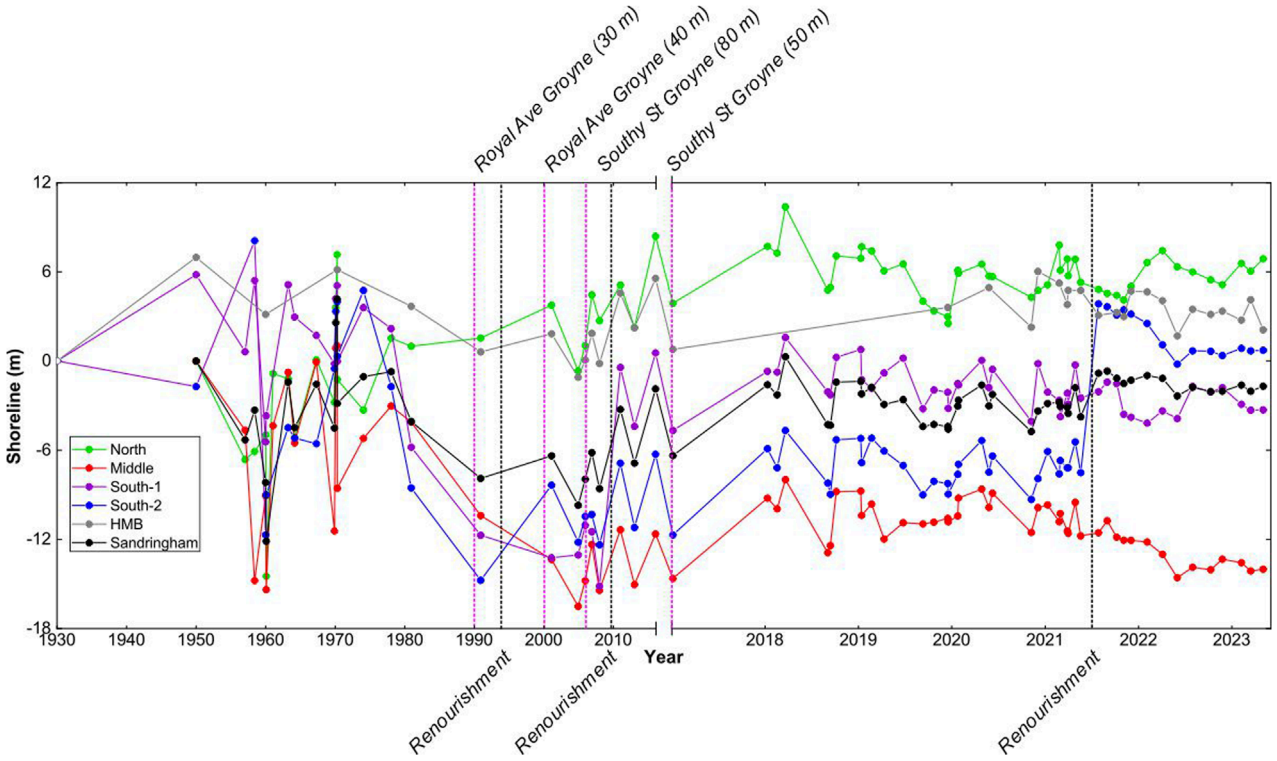

FIGURE 4
Long-term average shoreline position of the entire Sandringham Beach and each of its sub-compartments identified based on the aerial images (wetted line proxy) and UAV data (0.5 m AHD proxy) from 1930 to 2023. Three major nourishment and groyne building exercises are indicated by dashed lines. NB: for illustrative purposes the scale is changed post 2017, to show the more detailed shoreline trends observable in the higher resolution UAV data.

TABLE 2 The position of the wetted-line defined shoreline for those profiles in each sub-compartment with the largest seasonal variation.

Compartment (profile #)	Minimum position	Maximum position	Lateral variation (m)	Mean shoreline change
North (109)	−24	6.2	30	−0.74
Middle (67)	−20	−5.1	15	−3.0
South-1 (59)	−10	15	26	−2.1
South-2 (47)	1.9	25	23	+5.9
HMB (27)	−11	1.7	13	−1.27

Data based on UAV, shorelines from 4/12/2020 to 4/5/2023 and measured with respect to the 2019 DEA, shoreline. The mean shoreline change rate is calculated as a linear regression through the entire time period. All data is reported to two significant figures.

1980's after which they tended to be only a few metres between datasets. There is a possibility that the apparent dynamism of the older shorelines is a result of data availability and lower quality of the earlier images. It is also possible that short-term trends in shoreline movement may be causing the apparent spikes in shoreline position in the older time periods, especially as these occur during the period of major hard rock wall construction throughout the embayment.

For all of Sandringham Beach, the wetted shoreline tended to remain stable over long-term scale but accretes at the medium-term scale, with a short period of shoreline retreat and subsequent recovery centred around the 1990's (Figure 4; Table 2). The different patterns in change trend were reflected from most sub-compartments (e.g., Middle, South-1 and South-2) with erosion being dominant on the long-term but accretion was dominant at medium-term scale. In comparison, North and HMB showed

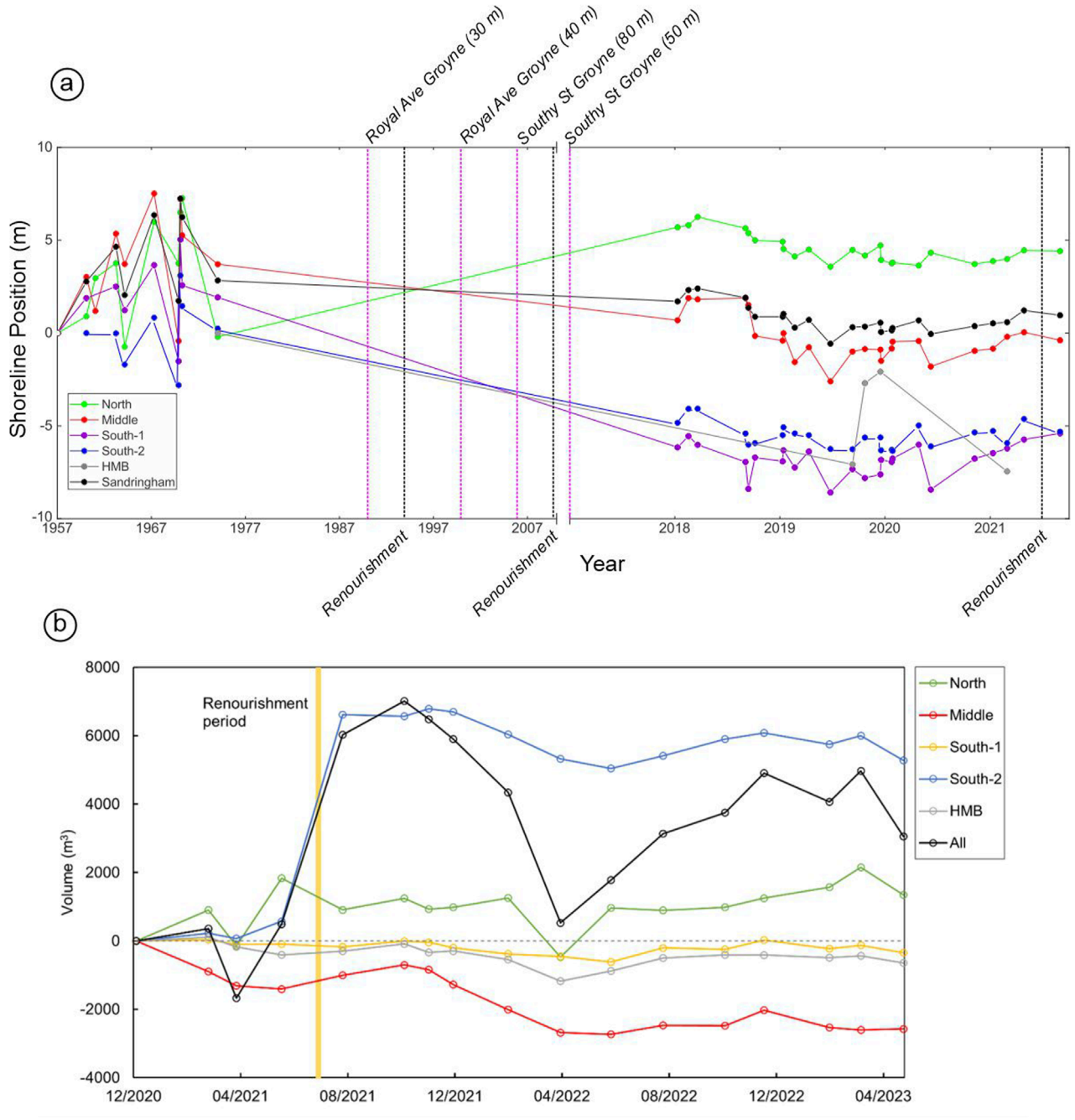

FIGURE 5
(a) Long-term shoreline position changes of Sandringham beach and each sub-compartment identified from aerial images based on the vegetated line from 1957 to 2021. Each point represents the average of all positions from each transect contained within each sub-compartment. Three major management exercises are indicated by dashed lines. The progradation of the shoreline at Half Moon Bay requires further investigation and likely is related to dune grass or annual species such as *Cackile* sp. growing on the beach. The shadowing of the beach by the backing cliffs inhibited accurate extraction of this proxy between 1970 and 2021. NB: for illustrative purposes the scale is changed post 2017, to show the more detailed shoreline trends observable in the higher resolution UAV surveys. **(b)** Volumetric change above 0.5 m AHD along the Sandringham Beach Embayment, capturing the addition of sand during the 2021 nourishment and the subsequent redistribution of the material throughout each sub-compartment over 2 years. "All" represents all the sub-compartments excluding Half Moon Bay (HMB).

an accretionary or stable trend over the long-term scale. The average shoreline change trend for Sandringham was accretionary due to nourishment at South-2 while erosion occurred in other sub-compartments (Table 2).

The vegetated line within the embayment can be considered to be representative of the long-term position of the sub-aerial, non-beach shoreline. The area immediately behind the beach, at present, is a mix of seawalls and cliffs mantled with natural and artificial talus.

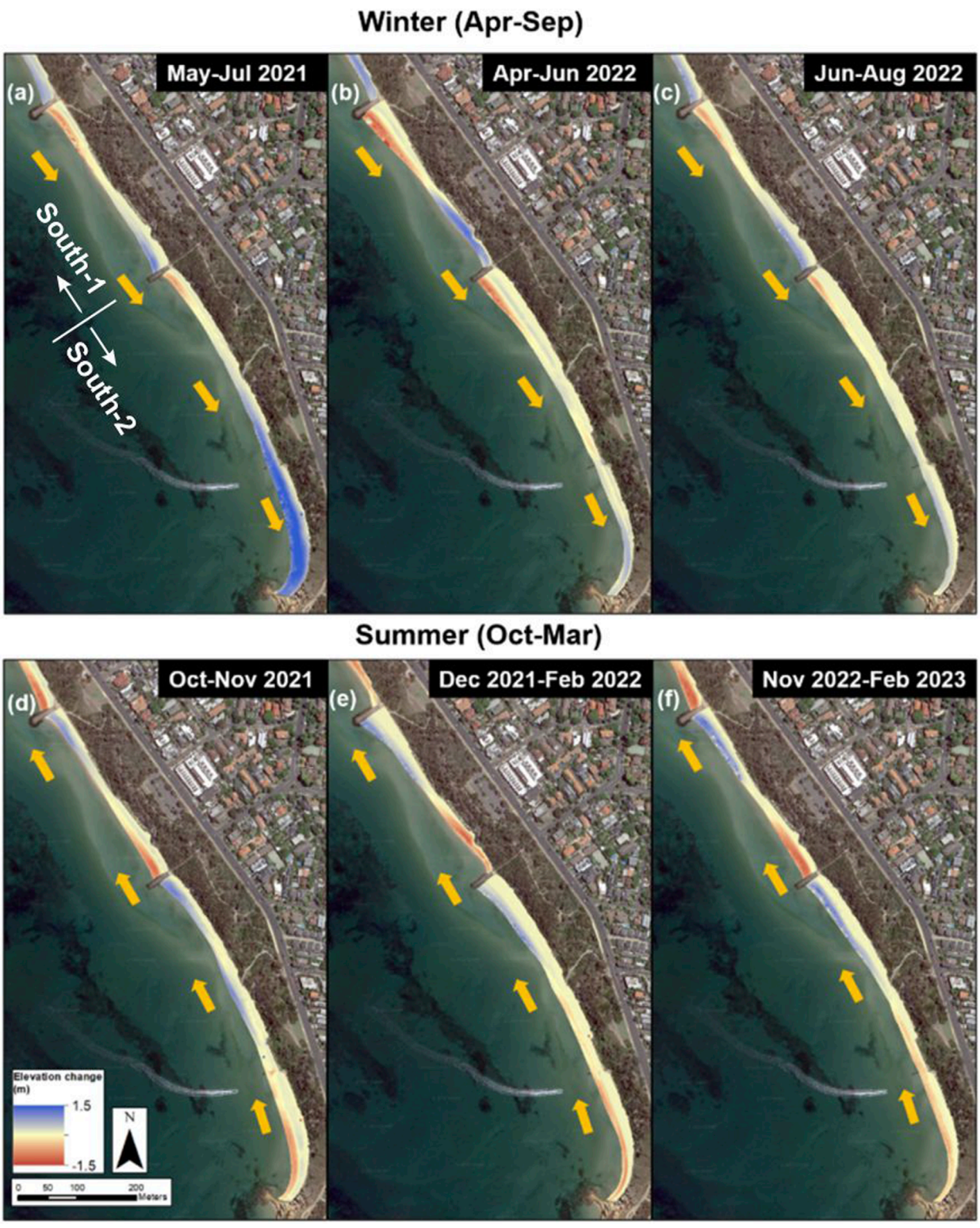

FIGURE 6
Examples of spatial patterns of seasonal shoreline change (since 2020) for the South-1 and South-2 sub-compartments which received significant nourishment in 2021. Analysis is based on UAV surveys. Lateral shoreline progradation and retreat is represented by the spatial extent of the respective colour ramps. Areas with no red-blue colour ramp are stable during the represented temporal scale. The DEM changes are represented for the periods **(a)** May-July 2021, **(b)** April to June 2022, **(c)** June to August 2022, **(d)** October to November 2021, **(e)** December 2021 to February 2022, and **(f)** November 2022 to February 2023.

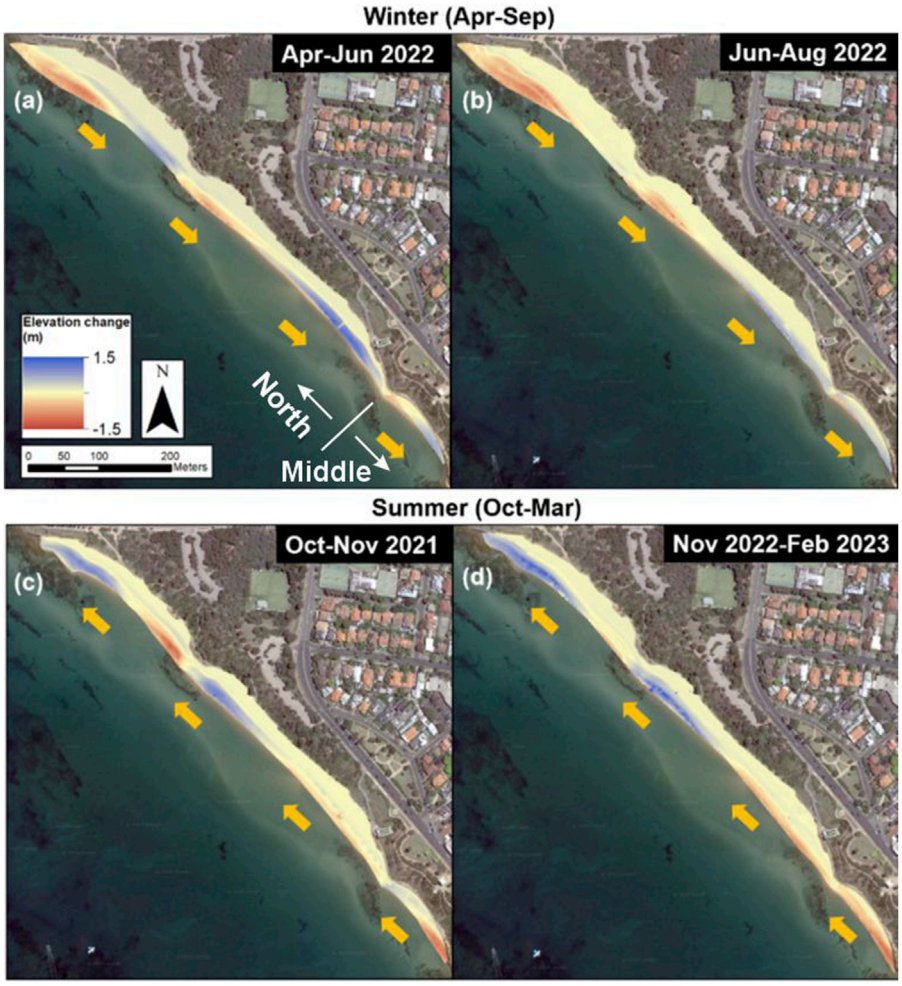

FIGURE 7
Examples of spatial patterns of seasonal shoreline change (since 2020) for the North sub-compartment which has generally accreted over the past 93 years. Analysis is based on UAV surveys. Lateral shoreline progradation and retreat is represented by the spatial extent of the respective colour ramps. Areas with no red-blue colour ramp are stable during the represented temporal scale. The DEM changes are represented for the periods **(a)** April to June 2022, **(b)** June to August 2022, **(c)** October to November 2021 and **(d)** November 2022 to February 2023.

The results in a floral community characterised predominately by shrubs and bushes with very minor grass colonisation (Figure 2). There was a slight overall erosion trend (−0.05 m/yr, p-value <0.001) for Sandringham Beach based on the vegetated line proxy from 1957 to 2021, with significant erosion observed at Middle, South-1 and South-2 sub-compartments (−0.07 m/yr, p-value <0.001; −0.16 m/yr, p-value <0.001; −0.11 m/yr, p-value = 0.001) (Figure 5a) (Table 2). In contrast, a significant slow accretion trend occurs in the North sub-compartment (0.03 m/yr, p-value = 0.01). The magnitude of change of the vegetation line varied from −8 to 7 m between 1957 and 1974, while reduced to ±2 m between 2018 and 2021 (Figure 5a).

4.4 Seasonal shoreline dynamics

Based on the monthly-scale UAV surveys, the beach exhibited strong seasonal fluctuations in shoreline position and elevation (Figure 6). Digital surface models show vertical change of around 1.5 m at the northern and southern ends of each sub-compartment (Figures 6, 7). On average, the northern end of beach was 30 m wider than the southern end within each sub-compartment. At southern end of the Sandringham Beach (sub-compartments South-1 and South-2) embayment, the beach widened and narrowed seasonally by up to 30 m on either side of the rock groynes. During the winter period (Apr-Sep), the dominant direction of longshore sediment movement was north to south, causing erosion at the northern end of sub-compartments (south side of groynes) and accretion at the southern end of sub-compartments (north side of groynes). The opposite trend occurred during summer. A similar pattern of seasonal change is also found around intertidal rocky outcrops at the northern end of the beach (Figure 7). The greatest amount of beach accretion was found at the south end of South-2 between May and July 2021 caused by the nourishment during a period of southerly longshore drift (Figure 6a).

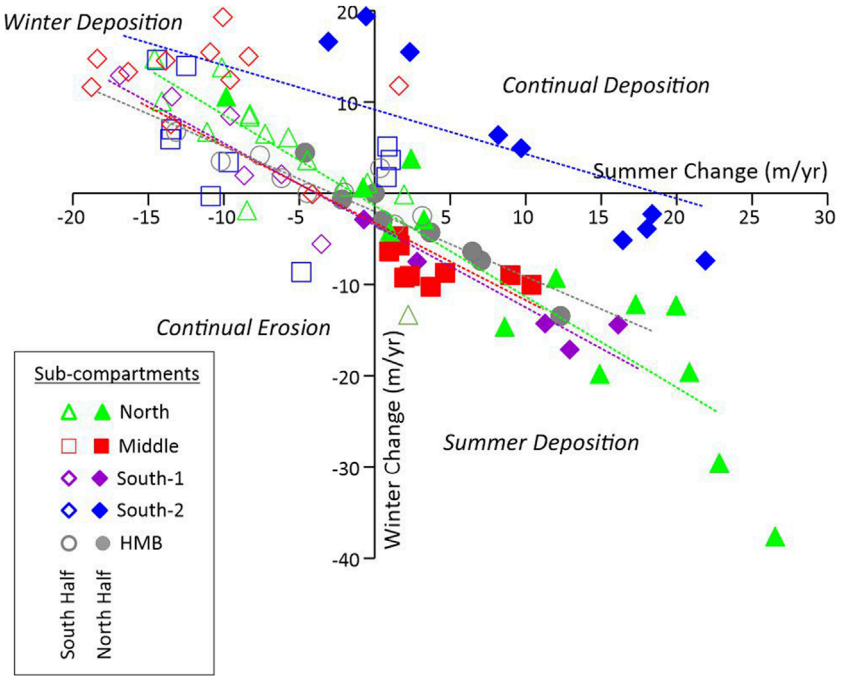

FIGURE 8
The seasonal shoreline dynamics between 2020 and 2023 of each sub-compartment can be observed through the variation in the rates of shoreline change as measured on each 30 m transect along the entire Sandringham Embayment. Each transect was classified as 'north' or 'south' based on its position relative to the midpoint within the sub compartment. The majority of transects are characterised by either winter or summer deposition. The dashed lines represent a linear regression for each sub-compartment. The sediment budgets in each sub-compartment are considered balanced when the linear regression passes through the origin, while being negative or positive when to the left or right of the origin respectively.

At the individual transect scale, the rate of shoreline change varied seasonally from +/- 20 m per year in the southern parts of each sub-compartment to +30/−40 m/yr at their northern ends (Figure 8). The northern areas accreted during summer and eroded during winter, while in the southern half the reverse pattern occurred (Figure 8). The transfer of sediment within each sub-compartment was almost evenly balanced (North) or had a very minor net deficit (Middle, South-1 and HMB) (Figure 8). Only South-2 varies from this pattern, with a net positive sediment budget. Here, significant accretion occurred in winter throughout the sub-compartment, except at its northern end. This distinctly different seasonal trend is attributed to the nourishment exercise undertaken in the winter of 2021, when the net direction of sediment movement was southerly.

4.5 Cross sectional beach dynamics

Overall, the beachface profiles, as observed through cross sections, are generally reflective in nature with the steep slopes (6.5°) characterising the intertidal zone (Figure 9). The beach generally terminated, at the landward end, at around 2 m above mean sea level (MSL), where it intersected either hard infrastructure or cliff slopes. Overall, across the entire embayment, the top of the beach berm, the limit of wave deposition was found at an elevation of between 1.5 and 2.0 m above MSL. The active beach envelope (excluding the renourished area (South-2)) for the last 3 years ranged between 10 and 25 m laterally and 1.0–1.5 m vertically, with HMB having the smallest envelope (Figure 9).

In the areas where the profile was most active, at the edges of the sub-compartments adjacent to the groyne structure, the mean variation in wetted-shoreline position ranged from 16.62 m (Middle) to 30.35 m (North). The average rate of change for the last 3 years was only positive in the renourished South-2 sub-compartment (5.97 m/yr) with the Middle sub-compartment retreating the most at −3.09 m/yr (Table 3).

5 Discussion

Sandringham Beach is a system that has been subjected to significant human intervention in the past 145 years (Cardno, 2016; Bird, 2011). The first phase of intervention prioritised the stability of the subaerial landscape rather than the beach. This occurred most intensively from the 1880's to 1950's when harbours/marinas and seawalls were built, the former being constructed at either end of the sediment compartment. Armouring of the cliff occurred concurrently with these activities. All these activities were detrimental to the beach sediment budget, through blocking sand supply from the subaerial cliffs and interrupting longshore transport. Effectively these activities changed the sediment compartment from being open to closed (sensu Thom et al., 2018). This management scheme led to shoreline retreat from 1960 up to the 1990's for the centre and southern ends of

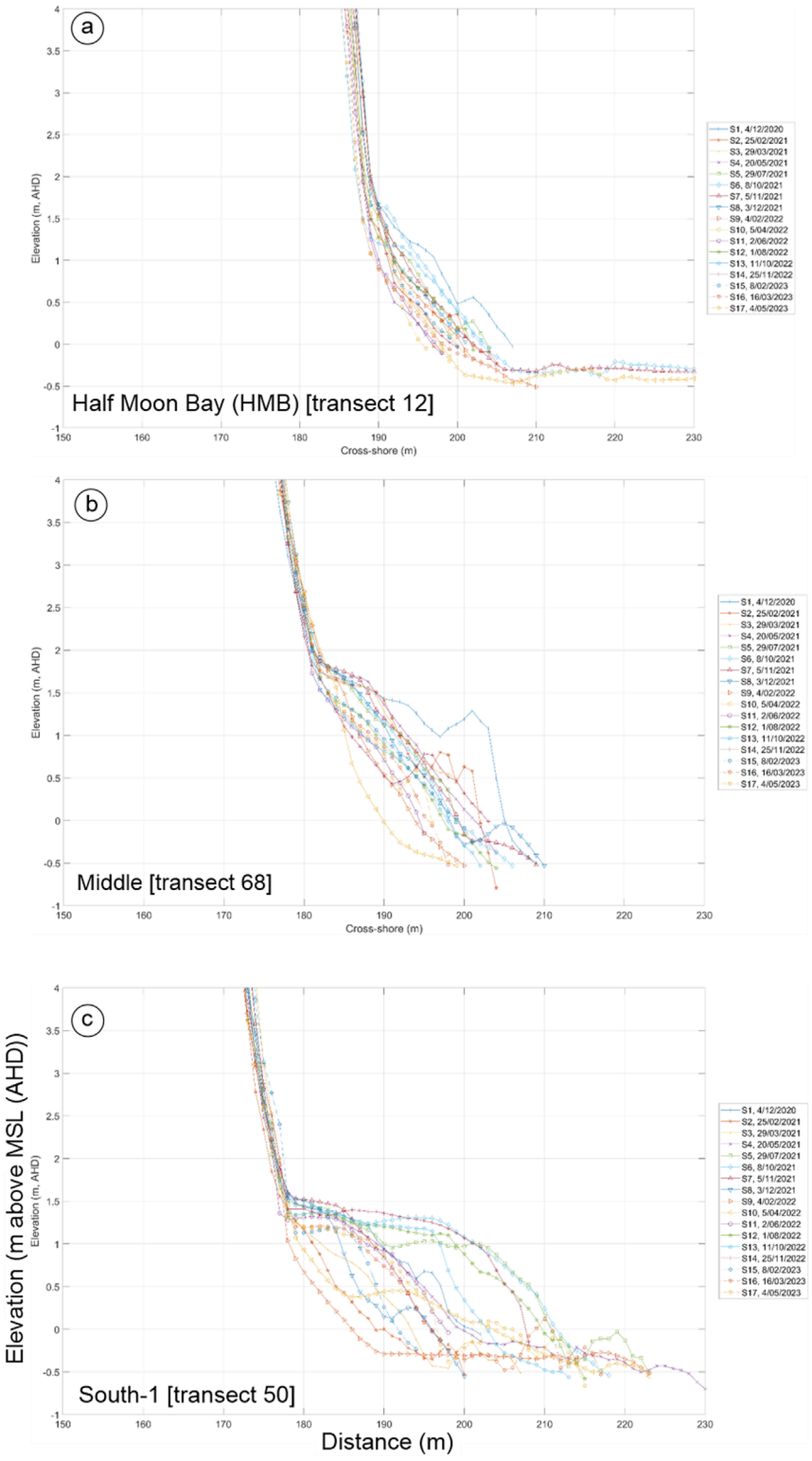

FIGURE 9
Beach profile dynamics along an example single transect **(a)** the southern end of Half Moon Bay, **(b)** the middle of the Middle, and **(c)** the southern end of South-1 sub-compartments to illustrate the change in profile position that occur over the seasonal scale.

10.3389/feart.2025.1607126

TABLE 3 Shoreline change trends over different timescales of each sub-compartment as indicated by wetted line and vegetated line.

Sub-compartment		North	Middle	South-1	South-2	HMB	Entire beach
Wetted Line							
1930–2023	Mean (m/yr)	0.1 ± 0.1	−0.1 ± 0.03	−0.1 ± 0.1	−0.0 ± 0.0	0.0 ± 0.1	0.0 ± 0.1
	p-value	<0.001	<0.001	0.01	0.2	0.6	0.4
1990–2023	Trend (m/yr)	0.2 ± 0.1	0.1 ± 0.1	0.5 ± 0.0	0.5 ± 0.1	0.1 ± 0.2	0.3 ± 0.2
	p-value	<0.001	0.12	<0.001	<0.001	<0.001	<0.001
2020–2023	Trend (m/yr)	0.2 ± 2.3	−1.8 ± 1.0	−0.6 ± 0.6	3.6 ± 1.7	−0.7 ± 1.8	0.50 ± 2.6
	p-value	0.4	<0.001	0.04	<0.001	0.02	0.03
Vegetation line							
1957–2021	Trend (m/yr)	0.0 ± 0.0	−0.1 ± 0.1	−0.2 ± 0.1	−0.1 ± 0.0	−0.11	−0.1 ± 0.1
	p-value	<0.001	<0.001	<0.001	<0.001	0.2	<0.001
2018–2021	Trend (m/yr)	−0.6 ± 0.6	−0.6 ± 0.3	0.0 ± 0.4	−0.2 ± 0.2	−2.26	−0.4 ± 0.5
	p-value	<0.001	0.01	0.6	0.2	0.5	0.01

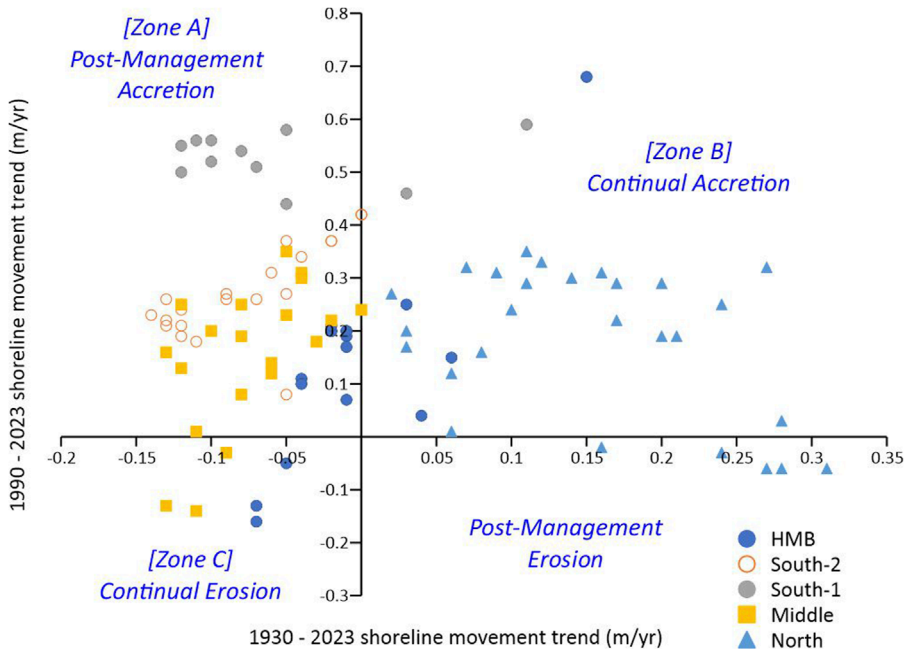

FIGURE 10
Shoreline change, based on the wetted-line proxy, trends per transect through the Sandringham Embayment. The trend from 1930 to 2023 represents the long term trajectory of shoreline movement (x-axis) while the 1990–2023 shoreline movement shows the trends under the current active management schemes (y-axis) Each sub-compartment distinctly clusters within three zones, Zone A where nourishment and groynes has caused accretion, Zone B where accretion has always occurred, and Zone C an area of long-term retreat.

Sandringham Beach, with some accretion at the northern end of the beach at the downdrift end of the longshore sediment transport system. Enhanced shoreline erosion due to seawall construction is common especially in estuarine settings (Nordstrom, 1989). The main period of shoreline recession occurs after 1980, preceded by a period characterised by large shoreline fluctuations (1950–1980). The large fluctuations preceding a period of sustained retreat may imply a sediment system not in equilibrium and therefore in a period

TABLE 4 Calculated sediment budget for the Sandringham Embayment.

Time period	1930–2023 (long term)	1990–2023 (medium term)	2020–2023 (short term)
Shoreline trend (m/yr)	0.02	0.25	0.50
Renourishment volume (m^3)	28,000	28,000	12,000
Natural volume (m^3)	1946	104,825	12,150
Rate of change (m^3/yr)	322	4,025	8,050

The embayment is 2.3 km long and the relief of the active profile from wave base to upper limit of swash is 7 m.

of adjustment to the major infrastructure construction activities being undertaken. While the total amount of retreat is low at Sandringham (−0.1 ± 0.1 m/yr based on the vegetation line since 1957), the narrow width of the beach meant it necessitated a change in management approach.

From 1990, groyne construction and nourishment became the primary management tool. This had the effect of progressively subdividing the tertiary compartment into smaller units (sub-compartments) (Figure 1). Seasonal rotation of the beach planform has been noted previously (Bird, 2011; Lowe and Kennedy, 2016), however the subdivision of the beach into smaller units made this adjustment quite pronounced (Figures 6, 7). The creation of the sub-compartments by 2006 saw the shoreline progressively widen until around 2018 where its position remained relatively stable. Groyne construction was accompanied by nourishment which assisted progradation and its impact of management can be observed in comparing the rates of shoreline change after 1990 (Table 2) (Figure 10). Sub-compartments which were previously eroding became accretionary (zone A). Only the North Sub-compartment is continually accreting as it is at the downstream end of the littoral drift system and has greater lateral accommodation space (Lowe and Kennedy, 2016).

Only one sub-compartment (Middle) shows continual erosion, except in the wetted line proxy 1990–2023 (Table 2). Here, the beach rests on top of an intertidal shore platform backed by a rocky cliff. The beach thickness here is low (<1 m), and this location likely operates more as a rocky shoreline with an ephemeral beach veneer (Kennedy and Milkins, 2015; Trenhaile, 2004). As rocky coasts are erosional in nature (Stephenson et al., 2013; Trenhaile, 1987) the long term retreat of this location is therefore not surprising.

As Sandringham Beach has undergone significant modification, it is necessary to differentiate between the natural and artificial sediment budgets to understand its future evolutionary trajectory. The sediment budget for the nourishment activities is based on reported volumes of sand added to the profile, though the accuracy of historical records is less than ideal. For sediment budget calculations, it is assumed that profile volume change is the product of shoreline change and active profile height (Dean and Houston, 2016; Rosati, 2005) (Equation 1) (Supplementary Table S1). This is generally a good assumption over longer time periods where longshore transport gradients are responsible for accretion/erosion. Conversely, this is a poor assumption where shoreline change is due alteration of the profile shape, e.g., soon after storms or nourishments. In the case of Sandringham, storm erosion is known to be minimal; however, total profile volume may be overestimated immediately following nourishments, until the profile shape re-adjusts (~1-year) (Beetham et al., 2023). Through this approach, the natural sediment budget for Sandringham Beach is slightly positive over the long term, but less than the nourishment volumes. On the short term (last 3 years) the natural volume change is almost the same as the nourishment volume (Table 4). The natural source of sand is most likely alongshore from adjacent compartments (Bird, 2011; Lowe and Kennedy, 2016; Kennedy et al., 2025) although an offshore source, from below 7 m depth, cannot be discounted (Dalby et al., 2024).

An alternate approach for understanding sediment budgets for the past 3 years can be taken through directly measuring volumetric change (Figure 5b). The UAV data shows that South-2 accreted by 6,433 m^3 post-nourishment representing 51% of the volume introduced by the contractor, the latter estimated by a pump delivery rate rather than direct measurement. The nourishment led to an increase of beach volume up to 7,007 m^3 when compared with December 2020. This material was then reworked by April 2022, but 93% returned in the summer of 2022–2023. Given the presence of extensive subtidal bars, sediment exchange between the subaerial and submarine components is to be expected (Short and Jackson, 2013). The variation in UAV-measured volume therefore likely relates to sediment exchange above and below mean sea level.

While the volumes measured from the UAV are less than those calculated from standard sediment budgets equations (Dean and Houston, 2016), given the different proxies and assumptions of the methods plus the UAV only measures subaerial change, the calculated longshore drift rates can be considered geomorphically similar. These rates (maximum 8,050 m^3/yr) (Table 4) are at the lower end of measured longshore transport rates of 3,600–13,300 m^3/yr on estuarine beaches with a 7–9 m wide active beachface exposed to a 15 km fetch at Fire Island New York, USA (Jackson et al., 2017; Nordstrom et al., 2003). The wave height on Fire Island was 0.1–0.3 m. A similar wave height also caused longshore drift rates of 12,000 m^3/yr on beaches 20 m wide in the Tagus Estuary Portugal (Freire and Andrade, 1999). The maximum H_s during the past 3 years at Sandringham Beach was 0.41 m and while slightly larger than those measured at Fire Island and Tagus Estuary, it is likely that the strong seasonal rotation drives the lower longshore transport rates at the entire compartment scale measured in this study. The rates at Sandringham Beach are however an order of magnitude less than those of open-ocean beaches such as Collaroy-North Narrabeen in eastern Australia which also undergoes major seasonal rotation of the planform profile (Harley et al., 2015).

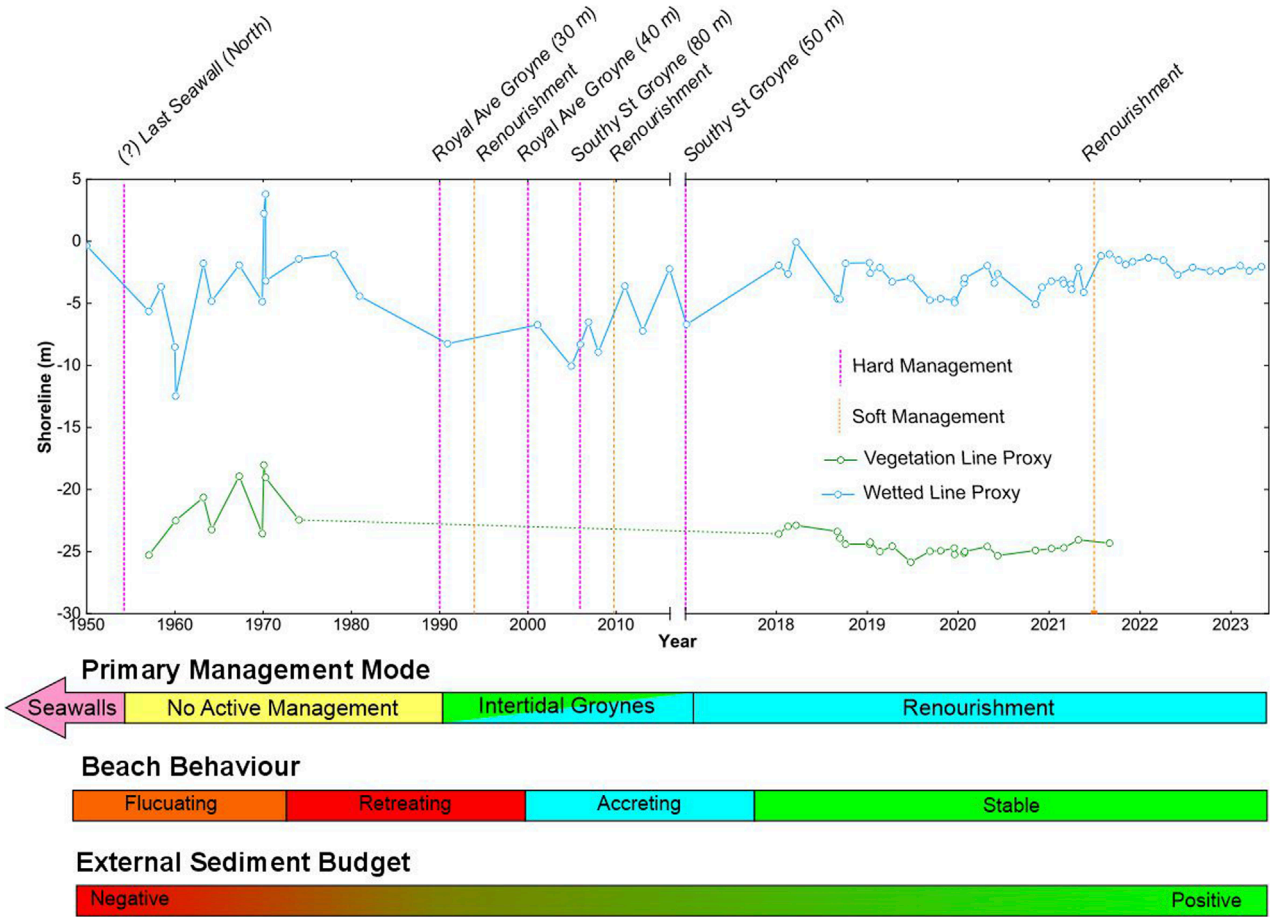

FIGURE 11
A summary of the shoreline trends at Sandringham Beach in association with changing management priorities, beach behaviour and associated sediment budgets.

The fluctuations in shoreline position and the associated sediment budget show that Sandringham Beach is mobile, with only a small sediment deficit (Figure 11). The recent nourishment program in 2021 had the most significant change on the shoreline dynamics acoss the entire beach, excluding the rocky sub-compartment. Associated with this shoreline dynamic has been a background rise of mean sea level within Port Phillip Bay of 4.8 mm in the past 29 years based on data from the Hovell Pile near the entrance to Port Phillip Bay (PSM, 2022) but the shoreline trends, at least at present, appear to be operating independently of this driver.

6 Conclusion

Sandringham Beach represents an important beach form, namely, a sandy system in a fetch-limited embayment removed from the influence of deepwater ocean swell. Such systems are found globally in large estuarine embayments and are commonly the location of significant urban development. Sandringham Beach, and much of the shoreline of Port Phillip Bay, is highly managed with beach nourishment having replaced hard armouring as the primary method of management of the sediment budget. The change in management schemes has been partly driven by a change in priorities from protection of the hinterland to maintenance of a functioning sedimentary system for recreation and as nature-based coastal defence.

It is found that management interventions on the beach have been a major driver of shoreline change in the past century. While seawalls initially reduced natural sediment supply, this has been balanced recently by nourishment programs (Figure 11). Of greatest significance to shoreline movement has been the subdivision of the tertiary-scale compartment into several sub-units through the construction of groynes. This subdivision has enhanced the seasonal rotation of the beach, by containing the sediments within small compartments which operate quasi-independently on a seasonal basis. This likely has had the effect of slowing the decadal-scale longshore migration of sand along the northeastern coastline of Port Phillip Bay. As nourishment now replaces the previously supply of sediment sourced from cliff erosion, the beach system can be considered as in an equilibrium state. Our findings show how understanding the sediment dynamics over seasonal to decadal

scales can lead to the sustainable management of the coastal environment.

Data availability statement

All data is available through the publicly accessible Victorian State Government, Department of Energy, Environment and Climate Action, Coastal Datashare Portal, https://datashare.maps.vic.gov.au/ The data can also be requested directly from the lead/corresponding author.

Author contributions

DK: Conceptualization, Data curation, Formal Analysis, Funding acquisition, Investigation, Methodology, Project administration, Resources, Supervision, Validation, Visualization, Writing – original draft, Writing – review and editing. RY: Data curation, Formal Analysis, Investigation, Methodology, Writing – original draft, Writing – review and editing. RM: Conceptualization, Formal Analysis, Funding acquisition, Investigation, Methodology, Project administration, Supervision, Writing – review and editing. JL: Data curation, Formal Analysis, Software, Writing – review and editing. EB: Formal Analysis, Validation, Writing – review and editing. DI: Conceptualization, Funding acquisition, Investigation, Methodology, Supervision, Writing – review and editing.

Funding

The author(s) declare that financial support was received for the research and/or publication of this article. This project was supported by funding from the Victorian Government Department of Energy, Environment, and Climate Action and Victorian Coastal Monitoring Program (VCMP) through the Sustainability Fund.

In memoriam

This paper is dedicated to the memory of Emeritus Professor Eric Bird who passed away in 2023 after a career dedicated, in part, to the beaches of Port Phillip Bay.

Conflict of interest

Author EB was employed by Tonkin and Taylor Ltd.

The remaining authors declare that the research was conducted in the absence of any commercial or financial relationships that could be construed as a potential conflict of interest.

Generative AI statement

The author(s) declare that no Generative AI was used in the creation of this manuscript.

Publisher's note

Supplementary material

The Supplementary Material for this article can be found online at: https://www.frontiersin.org/articles/10.3389/feart.2025.1607126/full#supplementary-material

References

Beetham, E., Perry, B., Mccarroll, J., Kennedy, D. M., Blakely, H., and Shand, T. (2023). "A multi-model workflow for assessing multi-scale beach dynamics," in *Australasian coasts and ports conference, 2023 Sunshine Coast, QLD*.

Bird, E. C. F. (1990). Artificial beach nourishment on the shores of Port Phillip Bay, Australia. *Journal of Coastal Research*. 6, 55–68

Bird, E. C. F. (2011). Changes on the coastline of Port Philip Bay. *Rep. Prep. Vic. Governement Dep. Sustain. Environ*. East Melbourne.

Bird, E., and Lewis, N. (2014). *Beach Renourishment*. Springer.

Bishop-Taylor, R., Nanson, R., Sagar, S., and Lymburner, L. (2021). Mapping australia's dynamic coastline at mean sea level using three decades of landsat imagery. *Remote Sens. Environ.* 267, 112734. doi:10.1016/j.rse.2021.112734

Bittencourt, A. C., Lessa, G. C., Dominguez, J. M., Martin, L., Vilas Bôas, G. S., and Farias, F. F. (2001). High and low frequency erosive and constructive cycles in estuarine beaches: an example from garcez point, bahia/brazil. *An. Acad. Bras. Ciências* 73, 599–610. doi:10.1590/s0001-37652001000400013

Boak, E. H., and Turner, I. L. (2005). Shoreline definition and detection: a review. *J. Coast. Res.* 21, 688–703. doi:10.2112/03-0071.1

Burningham, H., and Fernandez-Nunez, M. (2020). "Shoreline change analysis," in *Sandy beach morphodynamics*. Elsevier.

Cardno (2016). "Sandringham sand management scoping study," in *Report prepared for the department of environmental, land, water and planning*. Melbourne.

Carvalho, R. C., Kennedy, D. M., Niyazi, Y., Leach, C., Konlechner, T. M., and Ierodiaconou, D. (2020). Structure-from-motion photogrammetry analysis of historical aerial photography: determining beach volumetric change over decadal scales. *Earth Surf. Process. Landforms* 45, 2540–2555. doi:10.1002/esp.4911

Chen, W. L., Muller, P., Grabowski, R. C., and Dodd, N. (2022). Green nourishment: an innovative nature-based solution for coastal erosion. *Front. Mar. Sci.* 8, 814589. doi:10.3389/fmars.2021.814589

COASTKIT (2023). *CoastKit: Victoria's marine and coastal mapping portal [online]*. Department of Energy, Environment and Climate Action.

Costas, S., Alejo, I., Vila-Concejo, A., and Nombela, M. A. (2005). Persistence of storm-induced morphology on a modal low-energy beach: a case study from NW-Iberian peninsula. *Mar. Geol.* 224, 43–56. doi:10.1016/j.margeo.2005.08.003

Dalby, O., Kennedy, D. M., Mccarroll, R. J., Young, M., and Ierodiaconou, D. (2024). Mapping surface sediment characteristics in enclosed shallow-marine environments using spatially balanced designs and the random forest algorithm. *Earth Surf. Process. Landforms* 49, 2884–2897. doi:10.1002/esp.5864

DEA (2022). *Digital Earth Australia coastlines*. Geoscience Australia. Available online at: https://maps.dea.ga.gov.au/#share=s-DEACoastlines&playStory=1 (Accessed August, 2022).

DEA (2025). Digital Earth Australia shorelines: quality assurance. Available online at: https://knowledge.dea.ga.gov.au/data/product/dea-coastlines/?tab=quality (Accessed July, 2025).

Dean, R. G., and Houston, J. R. (2016). Determining shoreline response to sea level rise. *Coast. Eng.* 114, 1–8. doi:10.1016/j.coastaleng.2016.03.009

Fellowes, T. E., Vila-Concejo, A., Gallop, S. L., Schosberg, R., de Staercke, V., and Largier, J. L. (2021). Decadal shoreline erosion and recovery of beaches in modified and natural estuaries. *Geomorphology* 390, 107884. doi:10.1016/j.geomorph.2021.107884

Freire, P., and Andrade, C. (1999). Wind-induced sand transport in tagus estuarine beaches–first results. *Aquat. Ecol.* 33, 225–233. doi:10.1023/a:1009911012260

Gallop, S. L., Vila-Concejo, A., Fellowes, T. E., Harley, M. D., Rahbani, M., and Largier, J. L. (2020). Wave direction shift triggered severe erosion of beaches in estuaries and bays with limited post-storm recovery. *Earth Surf. Process. Landforms* 45, 3854–3868. doi:10.1002/esp.5005

Goodfellow, B. W., and Stephenson, W. J. (2005). Beach morphodynamics in a strong-wind Bay: a low-energy environment? *Mar. Geol.* 214, 101–116. doi:10.1016/j.margeo.2004.10.022

Hallermeier, R. J. (1980). A profile zonation for seasonal sand beaches from wave climate. *Coast. Eng.* 4, 253–277. doi:10.1016/0378-3839(80)90022-8

Hanson, H., Brampton, A., Capobianco, M., Dette, H. H., Hamm, L., Laustrup, C., et al. (2002). Beach nourishment projects, practices, and objectives—a European overview. *Coast. Eng.* 47, 81–111. doi:10.1016/s0378-3839(02)00122-9

Harley, M. D., Turner, I. L., and Short, A. D. (2015). New insights into embayed beach rotation: the importance of wave exposure and cross-shore processes. *J. Geophys. Res. Earth Surf.* 120, 1470–1484. doi:10.1002/2014jf003390

Harley, M. D., Masselink, G., Ruiz de Alegría-Arzaburu, A., Valiente, N. G., and Scott, T. (2022). Single extreme storm sequence can offset decades of shoreline retreat projected to result from sea-level rise. *Commun. Earth Environ.* 3, 112. doi:10.1038/s43247-022-00437-2

Ierodiaconou, D., Kennedy, D. M., Pucino, N., Allan, B. M., Mccarroll, R. J., Ferns, L. W., et al. (2022). Citizen science unoccupied aerial vehicles: a technique for advancing coastal data acquisition for management and research. *Cont. Shelf Res.* 244, 104800. doi:10.1016/j.csr.2022.104800

IUCN (2020). *Global standard for Nature-based solutions. A user-friendly framework for the verification, design and scaling up of NbS*. Gland, Switzerland: IUCN.

Jackson, N. L., Nordstrom, K. F., Eliot, I., and Masselink, G. (2002). Low energy sandy beaches in marine and estuarine environments: a review. *Geomorphology* 48, 147–162. doi:10.1016/s0169-555x(02)00179-4

Jackson, N. L., Nordstrom, K. F., and Farrell, E. J. (2017). Longshore sediment transport and foreshore change in the swash zone of an estuarine beach. *Mar. Geol.* 386, 88–97. doi:10.1016/j.margeo.2017.02.017

Kennedy, D. M. (2002). Estuarine beach morphology in microtidal middle harbour, Sydney. *Aust. Geogr. Stud.* 40, 231–240. doi:10.1111/1467-8470.00176

Kennedy, D. M., and Milkins, J. (2015). The formation of beaches on shore platforms in microtidal environments. *Earth Surf. Process. Landforms* 30, 34–46. doi:10.1002/esp.3610

Kennedy, D. M., Mccarroll, R. J., Fellowes, T. E., Gallop, S. L., Pucino, N., Mcsweeney, S. L., et al. (2023). Drivers of seasonal and decadal change on an estuarine beach in a fetch-limited temperate embayment. *Mar. Geol.* 463, 107130. doi:10.1016/j.margeo.2023.107130

Kennedy, D. M., Mccarroll, R. J., Provis, D., Mccowan, A., and Zavadil, E. (2025). Delineating sediment compartment boundaries in an urbanised embayment for geomorphic management of decadal-scale coastal dynamics. *Geomorphology* 477, 109702. doi:10.1016/j.geomorph.2025.109702

Lowe, M. K., and Kennedy, D. M. (2016). Stability of artificial beaches in port phillip Bay, Victoria, Australia. *J. Coast. Res.* 75, 253–257. doi:10.2112/si75-51.1

Mccarroll, R. J., Masselink, G., Valiente, N. G., Scott, T., Wiggins, M., Kirby, J.-A., et al. (2021). A rules-based shoreface translation and sediment budgeting tool for estimating coastal change: shoretrans. *Mar. Geol.* 435, 106466. doi:10.1016/j.margeo.2021.106466

Mccarroll, R. J., Kennedy, D. M., Liu, J., Allan, B., and Ierodiaconou, D. (2024). Design and application of coastal erosion indicators using satellite and drone data for a regional monitoring program. *Ocean and Coast. Manag.* 253, 107146. doi:10.1016/j.ocecoaman.2024.107146

Morris, R., Strain, E. M., Konlechner, T. M., Fest, B. J., Kennedy, D. M., Arndt, S. K., et al. (2019). Developing a nature-based coastal defence strategy for Australia. *Aust. J. Civ. Eng.* 17, 167–176. doi:10.1080/14488353.2019.1661062

Nordstrom, K. F. (1989). Erosion control strategies for Bay and estuarine beaches. *Coast. Manag.* 17, 25–35. doi:10.1080/08920758909362072

Nordstrom, K. F. (1992). *Estuarine beaches*. Elsevier Applied Science.

Nordstrom, K. F., and Jackson, N. L. (2012). Physical processes and landforms on beaches in short fetch environments in estuaries, small Lakes and reservoirs: a review. *Earth-Science Rev.* 111, 232–247. doi:10.1016/j.earscirev.2011.12.004

Nordstrom, K. F., Jackson, N. L., Allen, J. R., and Sherman, D. J. (2003). Longshore sediment transport rates on a microtidal estuarine beach. *J. Waterw. Port, Coast. Ocean Eng.* 129, 1–4. doi:10.1061/(asce)0733-950x(2003)129:1(1)

Pajak, M. J., and Leatherman, S. (2002). The high water line as shoreline indicator. *J. Coast. Res.*, 329–337. Available online at: https://www.jstor.org/stable/4299078

POM (2013). *Victorian tide tables, 88th edn*. Melbourne: Port of Melbourne Corporation.

PSM (2022). Permanent service for mean sea level. Available online at: https://psmsl.org/data/obtaining/stations/1777.php.

Pucino, N., Kennedy, D. M., Carvalho, R. C., Allan, B., and Ierodiaconou, D. (2021). Citizen science for monitoring seasonal-scale beach erosion and behaviour with aerial drones. *Sci. Rep.* 11, 3935. doi:10.1038/s41598-021-83477-6

Rosati, J. D. (2005). Concepts in sediment budgets. *J. Coast. Res.* 2005, 307–322. doi:10.2112/02-475a.1

Short, A., and Jackson, D. (2013). Beach morphodynamics. *Treatise Geomorphol.* 106–129. doi:10.1016/B978-0-12-374739-6.00275-X

Stephenson, W. J., Dickson, M. E., and Trenhaile, A. S. (2013). "Rock coasts," in *Coastal geomorphology*. Editor D. SHERMAN (San Diego: Academic Press).

Tran, H. Q., Provis, D., and Babanin, A. V. (2021). Hydrodynamic climate of port phillip Bay. *J. Mar. Sci. Eng.* 9, 898. doi:10.3390/jmse9080898

Trenhaile, A. S. (1987). *The geomorphology of rock coasts*. Oxford: Clarendon Press.

Trenhaile, A. S. (2004). Modeling the accumulation and dynamics of beaches on shore platforms. *Mar. Geol.* 206, 55–72. doi:10.1016/j.margeo.2004.03.013

Vandenberg, A. H. (2016). Depositional facies and extent of the late Neogene sandringham sandstone in southern Victoria, Australia. *Proc. R. Soc. Vic.* 128, 7–24. doi:10.1071/rs16009

Vila-Concejo, A., Gallop, S. L., and Largier, J. L. (2020). "Sandy beaches in estuaries and bays," in *Sandy beach morphodynamics*. Elsevier.

Vila-Concejo, A., Fellowes, T. E., Gallop, S., Alejo, I., Angnuureng, D. B., Benavente, J., et al. (2024). Morphodynamics and management challenges for beaches in modified estuaries and bays. *Camb. Prisms Coast. Futur.* 2, e11. doi:10.1017/cft.2024.7

Westoby, M., Brasington, J., Glasser, N., Hambrey, M., and Reynolds, J. (2012). Structure-from-motion photogrammetry: a low-cost, effective tool for geoscience applications. *Geomorphology* 179, 300–314. doi:10.1016/j.geomorph.2012.08.021